

Infrared and Raman Spectra of Macrocyclic Poly(oxymethylene)

Masamichi Kobayashi,*† Mami Sakashita,† and Masaki Hasegawa‡

Department of Macromolecular Science, Faculty of Science, Osaka University, Toyonaka, Osaka 560, Japan, and Department of Synthetic Chemistry, Faculty of Engineering, The University of Tokyo, Hongo, Bunkyo-ku, Tokyo 113, Japan

Received December 31, 1990

ABSTRACT: Infrared and Raman spectra of macrocyclic poly(oxymethylene) (MC-POM) samples having $\bar{M}_n = 1090$ have been investigated in relation to the unusually large and specific frequency shifts of the A_2 infrared bands of linear POM accompanied by the change in morphology from the extended-chain crystal (ECC) to the folded-chain crystal (FCC). The MC-POM sample deposited from solution gives rise to an IR spectrum having the A_2 bands at frequencies very close to those of FCC of linear POM. The A_2 bands of melt-crystallized MC-POM are red-shifted compared to those of the solution-deposited sample in a similar manner, but with smaller band shifts. The E_1 IR bands as well as the Raman-active A_1 and E_2 bands of MC-POM are essentially the same as those of linear POM (both ECC and FCC) regardless of the sampling process, indicating that the stems of the macrocyclic molecule assume the same (9/5)-helical conformation as that of linear POM. The LAM-1 Raman band of MC-POM is observed around 30 cm^{-1} as anticipated from the stem length (evaluated from \bar{M}_n) and the Young's modulus of the (9/5) helix (estimated by a spectroscopic method). The remarkably large dependence of the A_2 frequencies of MC-POM on the sampling process has been interpreted by the difference in the stacking mode of molecules among the samples. On compression, MC-POM is only weakly transformed to the metastable orthorhombic modification compared with linear POM.

Introduction

Poly(oxymethylene), $(\text{CH}_2\text{O})_n$ (abbreviated POM), is a well-known engineering plastic. It appears in two crystal modifications: the stable trigonal form (t-POM) and the metastable orthorhombic form (o-POM). The trigonal form consists of (9/5)-¹ or (29/16)-helical² molecules and is obtained exclusively through ordinary crystallization from the melt or from dilute solutions. The orthorhombic form consists of (2/1)-helical molecules.³ This form was first prepared by Mortillaro et al.⁴ through polymerization of formaldehyde in aqueous solution. Thereafter, Kobayashi, in collaboration with Iguchi et al., showed that o-POM is obtained as a byproduct of a heterogeneous cationic polymerization of trioxane which was originally designed for preparing needlelike single crystals of t-POM.^{5,6}

The trigonal form of POM is obtainable in various morphological structures between the two extreme cases of the fully extended-chain crystal (ECC) and the folded-chain crystal (FCC), depending on the methods of sample preparation and/or sample processing. A typical ECC sample is obtained through heterogeneous cationic polymerization of trioxane,^{7,8} giving micron-sized needlelike single crystals where the extended POM molecules align parallel to the needle axis. A typical FCC sample is obtained by crystallization from dilute solutions, giving hexagon-shaped lamellar crystals with a thickness of about 10 nm. The solution-grown powder sample is converted partly to an ECC type by rolling it at elevated temperature or by milling with KBr powder.

In a series of previous papers,⁹⁻¹² it was demonstrated that the vibrational spectrum of t-POM changes in a very specific manner with changing morphological structure. The infrared bands belonging to the A_2 symmetry species, having the transition dipole moment along the chain axis (the parallel bands), show a remarkable high-frequency shift as the sample goes from ECC to FCC. On the other hand, the E_1 bands, having the transition dipole perpen-

dicular to the chain axis (the perpendicular bands), as well as the Raman-active and infrared-inactive A_1 and E_2 bands appear at the same frequencies in both FCC and ECC samples. The same spectral change has been found in the case of o-POM samples which are converted from the ECC and FCC of t-POM through a pressure-induced phase transition.¹³ A series of t-POM oligomers having acetylated hydroxyl terminal groups gives rise to an infrared spectrum resembling that of FCC.¹⁴ This suggests that the characteristic feature of FCC is not ascribed to the folding structure, but to the short crystal dimension along the fiber axis. A similar but less significant spectral change has been observed for poly(ethylene oxide)^{15,16} and also for poly(tetrafluoroethylene).¹⁷

Thus, these very significant and specific spectral changes with changing crystal morphology are concluded to be not limited to the particular case of t-POM but to be generally observed for highly polar crystalline polymers. Although the origin of this very interesting phenomenon is not fully understood yet, the magnitude of the frequency shift of the A_2 IR band has been found to be proportional to its oscillator strength.^{13,18,19} This leads to the conclusion that the transition dipole interaction plays an important role in this phenomenon. Quantitatively, however, the observed shifts, which exceed 100 cm^{-1} for some strong bands, are large compared with the values estimated from the measured oscillator strengths through the theory of transition dipole-dipole interaction developed by Hexter.²⁰ Therefore, we have to search for another factor to be taken into account for the full explanation of this phenomenon. For this purpose, we need additional spectral data.

Recently, Hasegawa et al.²¹ succeeded in preparing macrocyclic POM samples with a narrow molecular weight distribution. These samples were isolated from alkaline-degraded bulk polymers synthesized by cationic polymerization of trioxane. They were very stable to alkaline degradation and exhibited no ^1H NMR signals due to terminal groups formed in cationic polymerization. They were therefore recognized to be of macrocyclic structure consisting of 50-70 monomeric units, judging from the

† Osaka University.

‡ The University of Tokyo.

Table I
Number of Normal Modes (n_j), Infrared and Raman
Selection Rules, and Polarizations of the (9/5)-Helical
Molecule of Trigonal POM [$D(10\pi/9)$]

species	n_j	infrared	Raman
A_1	5	forbidden	$(\alpha_{aa} + \alpha_{a'a'})$, α_{cc}
A_2	5	μ_c	forbidden
E_1	11×2	(μ_a, μ_a')	$(\alpha_{ac}, \alpha_{a'c})$
E_2	12×2	forbidden	$(\alpha_{aa} - \alpha_{a'a'}, \alpha_{aa'})$
E_3	12×2	forbidden	forbidden
E_4	12×2	forbidden	forbidden

averaged molecular weight of $\bar{M}_n = 1500$ –1680 or $\bar{M}_w = 1670$ –2070. Investigation of the infrared spectra of the macrocyclic oligomers might give us valuable information about the origin of the morphology-dependent frequency shift of the parallel bands, because these samples have morphologies quite different from those of linear POM. This is the main motive of the present work.

Secondly, we are concerned with convincing spectroscopic evidence indicating the macrocyclic structure and with structural changes occurring in the macrocyclic oligomers on various thermal and mechanical treatments.

In the present work, we are concerned with the infrared and Raman spectra of MC-POM samples, especially the spectral changes with change in morphological structure induced by various sample processing. All the experimental results are compared with those of linear POM embedded in both ECC and FCC.

Experimental Section

Samples. A sample of macrocyclic POM (MC-POM) was prepared and purified from hexafluoro-2-propanol (HFIP)/acetone (in Hasegawa's laboratory, University of Tokyo). It was characterized as follows: $\bar{M}_n = 1090$, $\bar{M}_w = 1710$, mp = 160 °C; the degradation temperature was 190 °C. The sample gave rise to an X-ray diffraction pattern (powder pattern) characteristic of the trigonal modification.²¹ For comparison, we reexamine a typical FCC sample [crystallized from a bromobenzene solution of Delrin resin (E. I. du Pont de Nemours)] and a typical ECC sample [needlelike crystals (whiskers) prepared by heterogeneous cationic polymerization of trioxane] of linear POM supplied by Dr. Iguchi of the Research Institute for Polymers and Textiles.

Spectral Measurements. Infrared spectra were taken with a JASCO 8000 type FT-IR spectrometer with a DTGS detector. Raman spectra were taken with a JASCO R-1000 double monochromator equipped with both a photomultiplier and an image sensor intensified multichannel detector (with 1024 channels). The 514.5-nm light from an Ar⁺ laser was used as the excitation source.

Results and Discussion

(1) Normal Vibrations of t-POM. The unit cell of t-POM contains one molecular chain having a uniform (9/5)-helical conformation in which nine monomeric units turn five times within the fiber identity period of 1.73 nm.¹ The molecule has the line group symmetry of $D(10\pi/9)$ (isomorphous with the D_9 point group), and the molecular vibrations (the optically active zone-center modes) are classified into six symmetry species A_1 through E_4 as described in Table I.²² The number of normal modes as well as infrared and Raman selection rules and polarizations for each species are given in the table. The A_2 modes are infrared-active and have the transition moment parallel to the chain axis, while the E_1 modes are active in both IR and Raman spectra and have the transition moment perpendicular to the chain axis. The A_1 and E_2 modes are Raman-active. There is only one chain per unit cell, so that no Davydov band splits are anticipated to be observed. As has been mentioned in a series of previous papers, the A_2 IR bands are very sensitive to the change in crystal

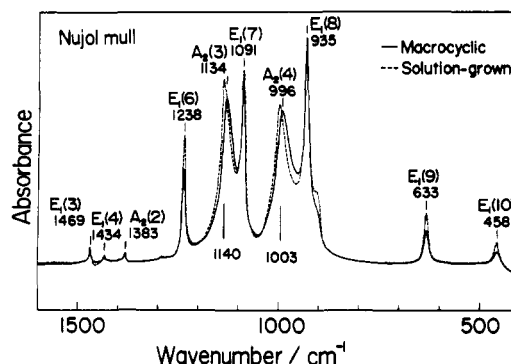


Figure 1. Infrared spectra of MC-POM deposited from a HFIP solution (—) and solution-grown (from bromobenzene solution) linear POM (---) measured on Nujol-mulled samples. The assignments of the fundamentals of the (9/5)-helical molecule are indicated.

morphology. Therefore, our attention is focused mainly on the behavior of the A_2 bands of MC-POM.

(2) Characteristic Features of the IR Spectrum of Macrocylic POM. The MC-POM sample as precipitated from HFIP/acetone (obtained as a fine powder) was milled with liquid paraffin (Nujol mull) and subjected to IR measurement. In the mulling process, special care was taken to prevent the original sample from structural changes induced by mechanical stress. In Figure 1, the IR spectrum (after subtracting the absorption due to liquid paraffin) thus obtained (solid line) is compared with that of a solution-grown sample of linear POM (abbreviated SG-POM) treated by the same mulling process (broken line). The assignments of the bands are indicated, with the numbering, from high to low frequency, of the fundamentals for each of the A_2 and E_1 species being described in parentheses.

As a whole, the two spectra are very similar and are typical of FCC type of linear POM.¹¹ However, the strong $A_2(3)$ and $A_2(4)$ bands are red-shifted by 6–7 cm^{-1} from the corresponding bands of SG-POM, while all the E_1 bands are unshifted. The Raman spectra of three POM samples, the needlelike crystals (ECC) and the solution-grown lamellar crystals (FCC) of linear POM and the solution-deposited sample of MC-POM, are compared in Figure 2. Here, the A_1 , E_1 , and E_2 modes are observed. The spectra in the 3100–400- cm^{-1} region are essentially the same for the three samples, except for the comparatively narrow bandwidths in ECC caused by its extremely high degree of crystal perfection. The MC-POM molecules in the present sample consist, on average, of about 40 monomeric units. The similarity in the Raman spectrum mentioned above tells us that the main part of the molecule assumes the same (9/5)-helical conformation as that of linear t-POM, though the stem length is as short as ~ 4.0 nm (Figure 3).

To check the polarization direction of the 1134- and 996- cm^{-1} bands of MC-POM, IR spectra were taken on samples with different plane orientations: the powder sample milled with liquid paraffin was sandwiched between two KBr windows with and without spacers of different thickness. As shown in Figure 4, the intensities of these bands relative to that of the 1091- cm^{-1} band $E_1(7)$ or the 935- cm^{-1} band $E_1(8)$ increase with an increase in the cavity thickness. This indicates that the polarization direction of the 1134- and 996- cm^{-1} bands tends to align perpendicular to the window surface as the cavity thickness decreases. A similar and more pronounced intensity change has been observed for the solution-grown lamellar crystals of linear POM (cf. Figure 5 in ref 11). This spectral

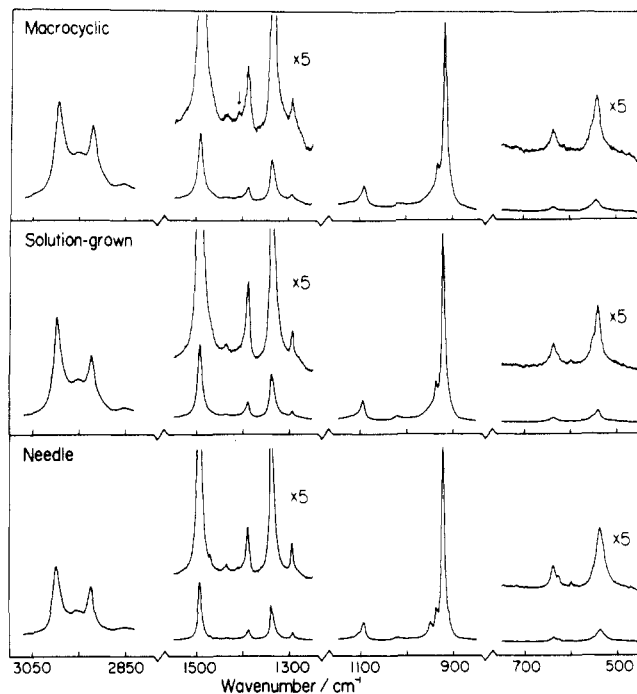


Figure 2. Raman spectra of MC-POM (deposited from a HFIP solution) (top), solution-grown FCC of linear POM (middle), and needlelike crystal (ECC) of linear POM (bottom).

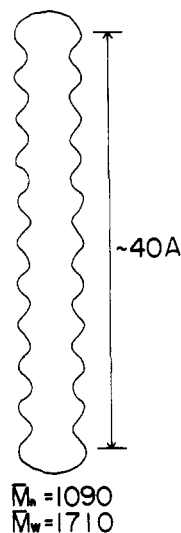


Figure 3. Molecular model of MC-POM.

change is accounted for by the preferred orientation of the lamellae: the fine lamellar crystals dispersed in liquid paraffin are aligned parallel to the window surface, with the molecular chains orienting perpendicular to it, when the mull is pressed between two optical windows, giving rise to the A_2 bands, which are weakened significantly in the IR spectrum taken with the normal incidence of radiation. In the thicker mulls put in the cavity supported by the spacer, the lamellae are more randomly oriented, causing a recovery of the A_2 band intensities. Thus, the present result suggests that the MC-POM sample deposited from HFIP solution has a lamellar morphology like the FCC of linear POM, although the lamellae are presumably not so uniform in thickness as in the latter case, judging from its less pronounced plane orientation.

When the solution-deposited sample of MC-POM was ground with KBr powder, the IR spectrum changed dramatically as shown in Figure 5: (1) the 1137- and 996- cm^{-1} bands shifted to 1103 and 920 cm^{-1} , respectively, (2) all the E_1 bands were weakened and broadened, and

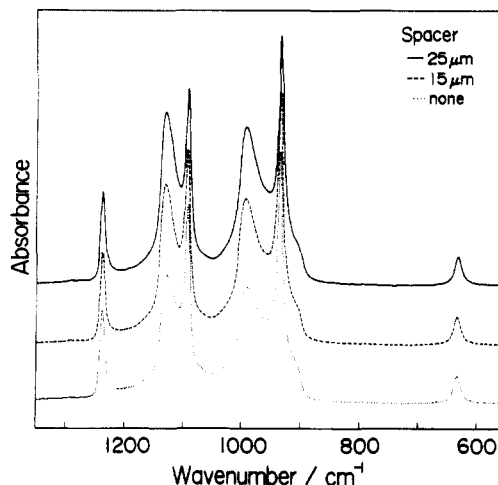


Figure 4. Infrared spectra of MC-POM (deposited from a HFIP solution) measured on Nujol-mulled samples with different thicknesses.

(3) broad bands appeared around 1495 and 1400 cm^{-1} which were due to the amorphous part. The spectral change is ascribed partly to the reduction in the degree of crystallinity accompanied by conformational disordering. When the ground sample is heated at 110 $^{\circ}\text{C}$ (below the melting point of MC-POM) and 180 $^{\circ}\text{C}$ (above the melting point) for 15 min and then cooled slowly to room temperature the intensities of the E_1 bands are restored and the amorphous bands are weakened by recrystallization of the sample. Especially, the intensity of the crystallization-sensitive band at 1238 cm^{-1} ²⁰ is restored to that of the starting sample (Figure 6). Moreover, the spectrum in the 1500–1350- cm^{-1} region resembles those of solution-grown and needlelike crystals (Figure 7). Nevertheless, the A_2 bands do not return to the starting profile; the 1103- and 920- cm^{-1} components still exist, and there appear broad shoulders around 1120 and 970 cm^{-1} .

On the basis of the IR and Raman spectral features mentioned above, the difference in the A_2 IR bands between the solution-deposited and melt-crystallized MC-POM samples is considered to be ascribed to different packing of macrocyclic molecules having the same stem conformation. Here, we mention the fact that the A_2 IR band profiles of the former sample are very close to those of SG-POM, which constructs a typical lamellar structure with a long spacing of ~ 10 nm. Therefore, it is assumed that in the solution-deposited sample, the macrocyclic molecules are so aligned that the (9/5)-helical stems construct the same trigonal lattice with an interstem distance of 0.446 nm as the case of linear POM, and the molecules are positioned at nearly the same height forming a lamellar-like structure as depicted in Figure 8a. The lamellar thickness of ~ 4 nm is only half or less of the case for SG-POM. The difference in the stem length, or the orderliness in the lamellar formation, seems to cause the difference in the A_2 band frequencies between the two cases.

The A_2 band profiles of the MC-POM sample ground with KBr and then annealed differ from those of any sample of linear POM treated by the same procedure (Figure 9). The most conspicuous difference is found in the low-frequency limit of the $A_2(4)$ band. The band appears at the lowest position of 897 cm^{-1} in the needlelike crystals (ECC) and shifts to 904 cm^{-1} in highly oriented linear POM or SG-POM well ground with KBr. In un-oriented or less oriented films, the $A_2(4)$ band spreads over a wide frequency range and two components are observed with rather broad peaks around 998 and 904

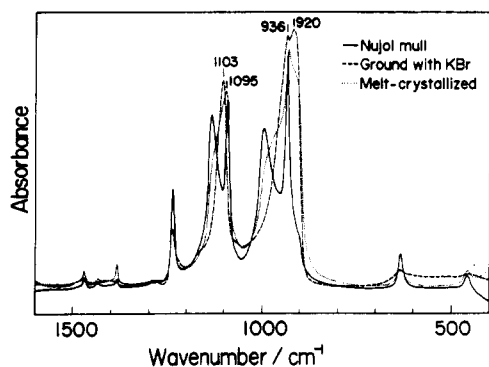


Figure 5. Infrared spectra of a MC-POM sample deposited from a HFIP solution after various processing: mullied with liquid paraffin (—); ground with KBr powder and pressed (---); melt-crystallized (···).

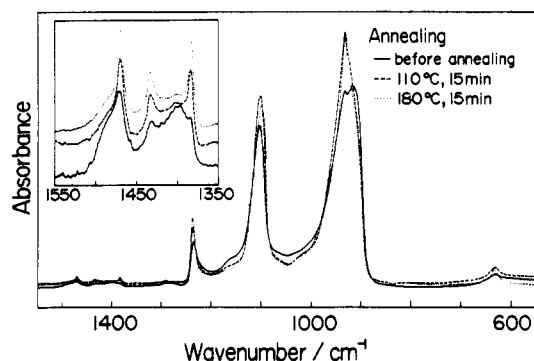


Figure 6. Change in infrared spectrum on annealing a MC-POM sample ground with KBr powder.

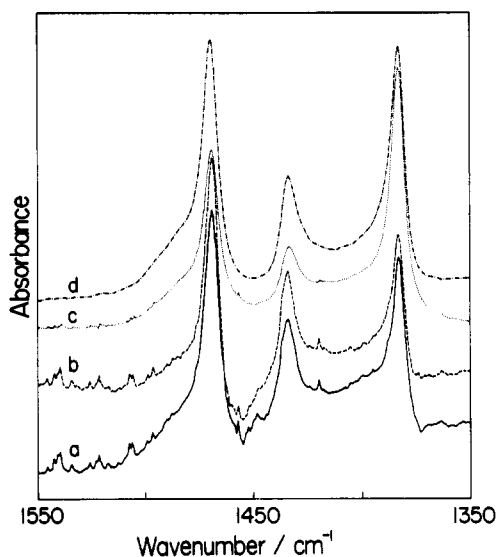


Figure 7. Infrared spectra in the CH_2 scissoring and wagging region of various trigonal POM samples: (a) MC-POM deposited from a HFIP solution; (b) FCC of linear POM; (c) melt-crystallized MC-POM; (d) ECC of linear POM.

cm^{-1} , the former and the latter corresponding, roughly speaking, to the folded and extended molecules. In MC-POM, on the contrary, extended chains cannot be formed by grinding with KBr powder. In fact, the low-frequency limit of the $\text{A}_2(4)$ band appears at 920 cm^{-1} , blue-shifted by 23 cm^{-1} from the position of the ECC sample.

In the case of linear POM, the remarkable frequency shifts of the A_2 modes accompanied by the change in morphology have been considered to originate mainly from strong transition dipole-dipole interactions induced along the POM chains by the in-phase vibrations of the molecules constructing lamellar crystallites, although the mecha-

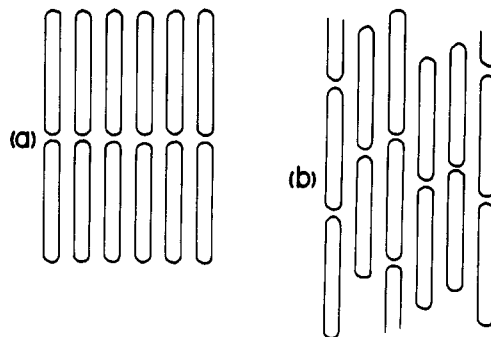


Figure 8. Models of molecular aggregation in MC-POM.

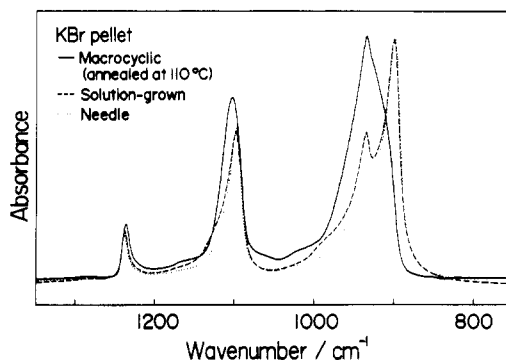


Figure 9. Comparison of the $\text{A}_2(3)$ and $\text{A}_2(4)$ IR bands among MC-POM (ground with KBr powder and then annealed) (—), a solution-grown sample of linear POM (ground with KBr powder) (---), and needlelike crystals (ECC) of linear POM (— · —).

nism is not fully understood. The origin of the similar but less significant band shifts found in MC-POM is rather difficult to understand, since the cyclic structure, i.e., the folding as an attribute of the molecule, should remain unchanged regardless of the sampling process. One possible interpretation is as follows. As described above, the MC-POM sample deposited from a HFIP solution seems to form a lamellar-like structure. In this case, the transition dipole interaction might be very close to the case of SG-POM, giving rise to similar IR spectra. In the melt-crystallized MC-POM, the molecules are supposed to pack in a nonlamellar fashion as described in Figure 8b. In such a case, the centers of the transition dipole are located at different heights, so that the resultant dipolar interactions on a particular helix stem differ from molecule to molecule depending on the locations of the surrounding molecules, giving rise to a broadened band profile of the $\text{A}_2(4)$ mode.

(3) Low-Frequency Raman Spectra of Macroscopic POM. The Raman spectra above 400 cm^{-1} of MC-POM and the ECC and FCC samples of linear POM are essentially the same, though they are different in the higher order structure. The difference is reflected in the low-frequency Raman spectrum (Figure 10). In this range there appear the $\text{E}_1(11)$ mode [the lowest E_1 fundamental of the (9/5)-helical molecule] and the so-called LAM-1 mode (the accordion-like vibration of the finite chain). The former appears at $64\text{--}65 \text{ cm}^{-1}$ in all three samples, while the sharpness is quite different among them, reflecting the difference in crystal order. The 41-cm^{-1} band of needlelike POM is unassigned.

The LAM-1 frequency depends on the stem length L , the density ρ , and the Young's modulus E of the molecule as expressed by the equation

$$\nu = (1/2cL)(E/\rho)^{1/2} \quad (1)$$

where c denotes the velocity of light in a vacuum.²³ The

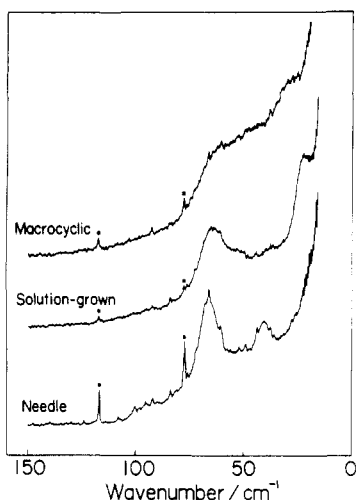


Figure 10. Low-frequency Raman spectra of MC-POM (deposited from a HFIP solution) (top), solution-grown (FCC) linear POM (middle), and needlelike ECC of linear POM (bottom). The sharp bands marked by asterisks are due to the nature emission from the laser.

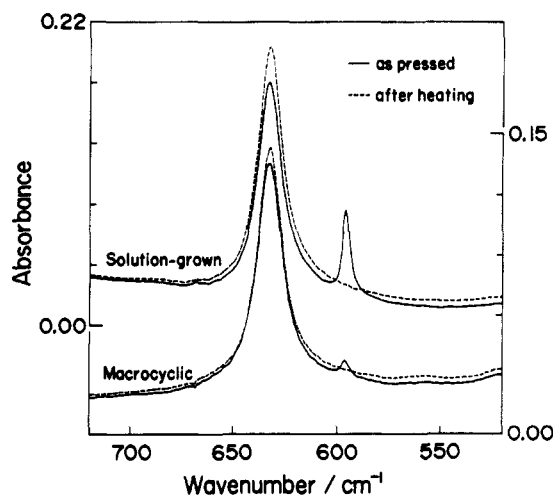


Figure 11. Infrared spectra of two trigonal POM samples partly transformed to the orthorhombic modification by compression (detected by the appearance of the 594-cm⁻¹ band in the solid curves) and the samples returned to the trigonal modification by heating (broken curves).

ρ of t-POM is 1.49 g cm⁻³, and E has been estimated as 109 GPa.²⁴ Therefore the relationship between ν (in cm⁻¹) and L (in nm) is

$$\nu = 1.43 \times 10^2 / L \quad (2)$$

In MC-POM (solution-deposited), there appears a very broad band centered at ~ 30 cm⁻¹. Estimating from \bar{M}_n and \bar{M}_w of the present MC-POM sample, the molecule has a stem length of 2.9–4.8 nm (assuming that three chemical units construct the fold parts), which corresponds to a LAM-1 frequency of 49–30 cm⁻¹. The broad profile may be due to the molecular weight distribution and disordering in the lamellar stacking. In SG-POM there appears a band at 21–22 cm⁻¹, which corresponds to a stem length of 6.8–6.5 nm (or a long spacing of 9.7–9.3 nm when the degree of crystallinity is 70%). In the needlelike crystal, no LAM-1 bands are observed down to 15 cm⁻¹, as anticipated from the ECC structure.

(4) Pressure-Induced Transition to the Orthorhombic Phase. It has been demonstrated that the trigonal phase of linear POM is partly (20 mol % or less) transformed to the metastable orthorhombic phase (o-POM) by compressing the powder sample.¹³ The resultant

orthorhombic phase is fully converted to the trigonal phase by heating the sample above 70 °C. The occurrence of these transformations is detected by the appearance and disappearance of the 594-cm⁻¹ band of o-POM (Figure 11). On compression of the MC-POM sample, the appearance of an orthorhombic phase is also detected, but the amount is very small compared to the case of linear POM. The GPC curve indicates that the present MC-POM sample may contain a trace of the high molecular weight component of linear POM.²¹ Therefore, it is likely that only the contaminating linear molecules transform to o-POM. The difficulty in the pressure-induced phase transition of the macrocyclic POM molecules is considered to come from the difficulty in constructing the orthorhombic unit cell (containing two chains passing through it) by one molecule consisting of two (2/1)-helical stems which should be correlated to each other by the $P2_12_12_1$ space group symmetry.³

Acknowledgment. We thank Dr. M. Iguchi of the Research Institute for Polymers and Textiles for kindly supplying the ECC sample. This work was supported by a Grant-in-Aid for Scientific Research on the Priority Area "New Functional Materials—Design, Preparation and Control", The Ministry of Education, Science and Culture, Japan (No. 02205086).

References and Notes

- (1) Tadokoro, H.; Yasumoto, T.; Murahashi, S.; Nitta, I. *J. Polym. Sci.* **1960**, *44*, 266. Uchida, T.; Tadokoro, H. *J. Polym. Sci., Polym. Phys. Ed.* **1967**, *5*, 63.
- (2) Carazzolo, G. A. *J. Polym. Sci., Part A* **1963**, *1*, 1573.
- (3) Carazzolo, G. A.; Mammi, M. *J. Polym. Sci., Part A* **1963**, *1*, 965.
- (4) Mortillaro, L.; Galliazzo, G.; Bessi, S. *Chem. Ind. (Milan)* **1964**, *46*, 139, 144.
- (5) Kobayashi, M.; Itoh, Y.; Tadokoro, H.; Shimomura, M.; Iguchi, M. *Polym. Commn.* **1983**, *24*, 38.
- (6) Iguchi, M. *Polymer* **1983**, *24*, 915.
- (7) Iguchi, M. *Br. Polym. J.* **1973**, *5*, 195.
- (8) Iguchi, M.; Murase, I.; Watanabe, K. *Br. Polym. J.* **1974**, *6*, 61.
- (9) Shimomura, M.; Iguchi, M. *Polymer* **1982**, *23*, 509.
- (10) Kobayashi, M.; Morishita, H.; Ishioka, T.; Iguchi, M.; Shimomura, M.; Ikeda, T. *J. Mol. Struct.* **1986**, *146*, 155.
- (11) Shimomura, M.; Iguchi, M.; Kobayashi, M. *Polymer* **1987**, *29*, 351.
- (12) Kobayashi, M.; Morishita, H.; Shimomura, M.; Iguchi, M. *Macromolecules* **1987**, *20*, 2453.
- (13) Kobayashi, M.; Morishita, H.; Shimomura, M. *Macromolecules* **1989**, *22*, 3726.
- (14) Shimomura, M.; Iguchi, M.; Kobayashi, M. *Polymer* **1990**, *31*, 1406.
- (15) Kobayashi, M.; Gu, Q.; Kaneko, F.; Iguchi, M.; Shimomura, M. *Polym. Prepr., Jpn.* **1984**, *33*, 2299.
- (16) Shimomura, M.; Tanabe, Y.; Watanabe, Y.; Kobayashi, M. *Polymer* **1990**, *31*, 1411.
- (17) Kobayashi, M.; Sakashita, M.; Kobayashi, M. *Rep. Prog. Polym. Phys. Jpn.*, in press.
- (18) Kobayashi, M.; Shimomura, M. *Polym. Prepr. Jpn.* **1989**, *38*, 919.
- (19) Kobayashi, M.; Sakashita, M. *J. Chem. Phys.*, to be published.
- (20) Hexter, R. M. *J. Chem. Phys.* **1960**, *33*, 1833; **1962**, *36*, 2285.
- (21) Hasegawa, M.; Yamamoto, K.; Shiwa, T.; Hashimoto, T. *Macromolecules* **1990**, *23*, 2629.
- (22) Tadokoro, H.; Kobayashi, M.; Kawaguchi, Y.; Kobayashi, A.; Murahashi, S. *J. Chem. Phys.* **1963**, *38*, 703.
- (23) Schaefele, R. F.; Shimanouchi, T. *J. Chem. Phys.* **1967**, *47*, 3605.
- (24) Wu, G.; Tashiro, K.; Kobayashi, M. *Macromolecules* **1989**, *22*, 758.